



DEVELOPMENT AND EVALUATION OF ACRONINE CO-DELIVERED TAMOXIFEN LOADED CHITOSAN NANOPARTICLES TO COMBAT CANCER

Pooja Khatkar^{*1}, Dr. Sanjeev Sharma² Suman³ and Vijeta Kumari⁴

Pooja Khatkar¹ - Department of Chemistry, Om Sterling Global University, Hisar, Haryana-125001, India

Dr. Sanjeev Sharma² - Department of Chemistry, Om Sterling Global University, Hisar, Haryana-125001, India

Suman³ - Assistant Professor, Department of Chemistry, Om Sterling Global University, Hisar, Haryana-125001, India.

Vijeta Kumari⁴ - Department of Chemistry, Om Sterling Global University, Hisar, Haryana-125001, India.

Corresponding Author*

Pooja Khatkar

Research Scholar

Department of Chemistry, Om Sterling Global University, Hisar-125001, Haryana, India.

E-mail-khatkarpooja94@gmail.com

Contact no. – +919729466599, +917988002818

Abstract

Chemotherapeutics approaches used to cure cancer are frequently faced a problem of drug resistances. Secondary metabolites of the plants having anticancer potency can be effectively raised by formulating them at nanoscale. Acronine is a natural alkaloid with an acridine structure isolated from the bark of the plant *Acronychia baueri* (Australian scrub ash) with antineoplastic properties. Acronine is an antitumor alkaloid with poor water solubility and low potency. Tamoxifen is a selective estrogen receptor modulator used to treat estrogen receptor positive breast cancer, reduce the risk of invasive breast cancer following surgery, or reduce the risk of breast cancer in high risk women. To improve the bioavailability and to generate synergetic effect, Acronine and TAM loaded Chitosan nanoparticles (ATCNPs) were synthesized by oil in oil (O/O) emulsion solvent evaporation techniques. The zeta potential value of ATCNPs was come out to be -45.9 mV representing relative stability of nanoparticles. The percentage encapsulation efficiency value was found to be 78.1% for Acronine and 78.4% for TAM. The ATCNPs possess particle size in the range of 55 – 78nm as revealed by TAM. SEM image analysis confirmed that the nanoparticles have spherical in shapes. The ATCNPs exhibited sustained release and their anti-oxidant and anti-cancer potency was much more pronounced than free Acronine and TAM particles alone. The *in vitro* studies demonstrated that Acronine and TAM encapsulated in dammar gum inhibited growth of A-549 cells, MCF-7 and Hela cell lines, respectively more effectively than Acronine and TAM alone which proved their robust anticancer potential.

Keywords: Chitosan, Acronine, Tamoxifen, Anti-cancer, Nanoparticles

Introduction

Nanotechnology in cancer treatment opens a new emerging area of pharmaceutical findings. Nanosized drug molecules provides novel highly potent bioactive loaded nanoplatform to fight cancer cells. Chemotherapy is frequently utilized to manage various cancers [1]. In contrast, these conventional curative approaches are linked to brutal effects, particularly drug tolerance or resistance [2,3]. Nanotechnology enabled solutions for life-threatening diseases are popular now-a-days. The bioactive agents at nanometric scale exhibit high bioavailability at low dose and enhanced antioxidant and anticancer potential. In USA, National Institute of Cancer has promoted the examination of the antitumor effect of many secondary metabolites of plants [4, 5]. Phytochemicals like boswellic acid and Betulinic acid (BA) have already reported in literature to exert cytotoxic effects [6]. Contemporary studies have shown that the morphological properties of nanoparticles are extremely important for attaining anticancer activity with fewer side effects [7]. The size, shape & surface traits of nanoparticles influence the pharmacokinetic as well as pharmacodynamic properties of nanoparticles.

Acronine have significant natural potency to combat various diseases because of their alkaloid nature [8]. Acronine exhibits diverse biological curative properties such as anti-inflammatory potential [9], hepatoprotective in nature [10], antioxidant action [11], antibacterial nature, antiviral activity [12] and anti-tumor actions [13]. But, its nonpolar hydrophobic nature and low solubility profile limit its clinical potential and efficiency [14]. However, improving drug release kinetics pattern of Acronine can render it beneficial in drug delivery potentials [15]. Due to its low level of toxicity, Acronine is generally used in pharmaceutical formulations that could be administered both orally & topically [11, 12].

Biodegradability & biocompatibility are ideal features considered for selection of an agent for encapsulating numerous drugs [13,14]. Chitosan is the only polycation in nature; novel encapsulation compound employed for therapeutic action and has shown proportional augmentation in encapsulation efficiency with increase in polymeric concentration [15]. It has antibacterial activity, non-toxicity, ease of modification and biodegradability. It is used as medicine and in drug manufacturing.

Tamoxifen (non-steroidal) is a type of hormonal therapy known as a selective estrogen receptor modulator (SERM). The drug attaches to hormone receptors (specific proteins) in breast cancer cells. Once the medication is inside the cells, it stops the cancer from accessing the hormones they need to multiply and grow [16,17]. Since the Food and Drug Administration (FDA) approved tamoxifen in 1998, it has become one of the most widely used in breast cancer treatments. It is a nonpolar molecule which acts by: (1) to compete with 17β -estradiol (E2) at the receptor site and to block the promotional role of E2 in breast cancer and (2) to bind DNA after metabolic activation and to initiate carcinogenesis. [18,19]. Its structural specificity with the cell membrane and adjuvant hormonal therapy provides anticancer activity [20].

In the present study, Acronine co-delivered TAM Chitosan nanoplatform were prepared with the aim to improve bioavailability, bring synergism and to overcome the side effects. The encapsulation of TAM and Acronine in the polymeric nanoparticles renders sustained release & higher therapeutic efficacy at low dosage.

Materials and Methods

Materials

Chitosan was purchased from MP Biomedicals, LLC, France. Acronine (>90%) and Tamoxifen were procured from Sigma Aldrich, India. Cell lines A-549 (Human lung adenocarcinoma epithelial cells), MCF-7 (Human breast adenocarcinoma cells) and Hela (Human cervical carcinoma cell line) were procured from National Center for Cell Science (NCCS), Pune. All the chemicals used in the present study were of analytical grade.

Preparation of Acronine & TAM loaded Chitosan nanoparticles (ATCNPs)

The ATCNPs were synthesized by oil in oil emulsion solvent evaporation method [21]. 150 mg of Chitosan, 40mg of Acronine and 5mg of TAM were dissolved in 100ml of Ethanol. 10 mg of Calcium stearate was added to the above solution and the resulting mixture was kept under magnetic stirring (1000 rpm) for 20min. 40 ml of liquid paraffin oil was poured slowly to the mixture with continuous stirring at 1000 rpm at 37° C for 12h and centrifuged at 7500 rpm, 4°C for 60 minutes. The pellet was isolated and suspended in cryoprotectant (D-Mannitol, 5% w/v) and freeze-dried.

Characterization of synthesized ATCNPs

Zetasizer Nano ZS-90 was used to assess the average size and size distribution (polydispersity index) of optimized nanoformulation of ATCNPs. After centrifugation at 7500 rpm (4°C) for 60 minutes, the supernatant having the unbound drug was collected and analyzed by UV spectra and encapsulation efficiency was calculated using following formula:

Percent Entrapment efficiency = (Total Drug-Unbound Drug/Total Drug) × 100

The size and morphology of optimized batch of ATCNPs was analyzed by transmission electron microscope. The FTIR analysis of Acronine, TAM, dammar Gum and BFDNPs was analyzed by Fourier transform infrared spectrophotometer in range of 4500–500 cm⁻¹.

In vitro release profile of ATCNPs

The dialysis sac method was used to study the release profile. 10 mg of Acronine co-delivered TAM loaded Chitosan nanoparticles were transferred to dialysis sac and positioned in water (10ml) and immersed in ethanol (25%) - phosphate buffer (0.1 M) saline pH 7.4 and constantly stirred at 100 rpm at a steady temperature of 37 °C [21]. One ml sample was withdrawn and collected at regular intervals of 1, 2, 3, 6, 12, and 24 h and examined by UV spectroscopy Acronine (210.7 nm, 6.43 min, TAM (256 nm, 7.89 min).

Antioxidant activity

The antioxidant potential of Acronine, TAM, Chitosan and ATCNPs was evaluated by 1,1-diphenyl-2-picrylhydrazyl (DPPH) assay [22]. DPPH is a free radical was homogenously mixed in methanol (3.9 mg/100 ml). Pure Acronine, TAM, Chitosan and ATCNPs were incubated along with DPPH for 30 min in dark condition to evaluate the inhibition of DPPH in triplicate run and the absorption peak was recorded using UV spectrophotometer at 517 nm. Blank Chitosan NPs were treated as a negative control while pure Acronine and TAM were used as positive control. The percentage inhibition of DPPH by pure Acronine, TAM and ATCNPs was calculated by formula as under:

$$\text{Percent antioxidant activity} = \frac{\text{Absorbance of control} - \text{Absorbance of sample}}{\text{Absorbance of control}} \times 100$$

In-vitro assay for cytotoxic activity (MTT assay)

Cell lines were raised in media supplemented with inactivated FBS (10%) solution, antibiotic streptomycin 80µl/ml with 80µl/ml penicillin concentration, incubated at 37°C temp, 5% CO₂ environment [21, 23]. The seeding of cells was experimented in 96 – well plates (10⁴ per 100µl per well). The growth kinetics pattern was analyzed to evaluate density of each cell line. For optimization the wells were treated after 8 h incubation with various concentration of ATCNPs (0.1-500µg/ml) & Acronine for three days (in triplicate). Subsequently, after raising cells, the medium was replaced by 2.5µl of MTT solution (5mg/ml) and incubated for 180 min. The percent of metabolically active cells were compared with untreated controls on the basis of the mitochondrial conversion of 3-(4, 5-dimethylthiazol-2-yl) 2, 5 diphenyltetrazolium bromide (MTT) to Formazan crystals. The formazan crystals were dissolved in DMSO and its absorbance was calculated by 96 wells microplate reader at 570 nm. The anticancer activity of ATCNPs was evaluated using pure Acronine and TAM as standard by MTT assay against cell lines A-549 cells, MCF-7 and Hela cell lines. The percentage cell growth inhibition (1) and percentage cytotoxicity (2) was calculated by following formula:

$$\% \text{viability} = (A_{Tr} - A_{Bl}) / (A_{Ct} - A_{Bl}) \times 100 \dots\dots\dots (1)$$

Where A_{Tr} = Absorbance for treated cells (drug); A_{Bl} = Absorbance for blank

A_{Ct} = Absorbance for control (untreated)

$$\% \text{cytotoxicity} = 100 - \text{Percent cell survival} (\%) \dots\dots\dots (2)$$

Results and Discussion

Particle size and Zeta Potential

The ATCNPs were analyzed for particle size and zeta potential. The ATCNPs size was found to be 220.6 nm (Fig 1) with zeta potential value of -45.9 mV (Fig 2), signifying relative stability of prepared nanoformulation.

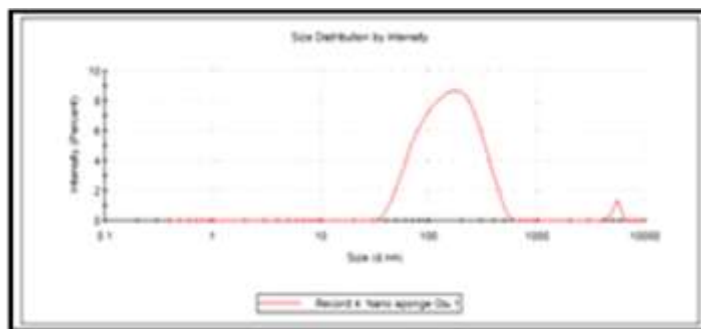


Figure 1. DLS image of ATCNPs

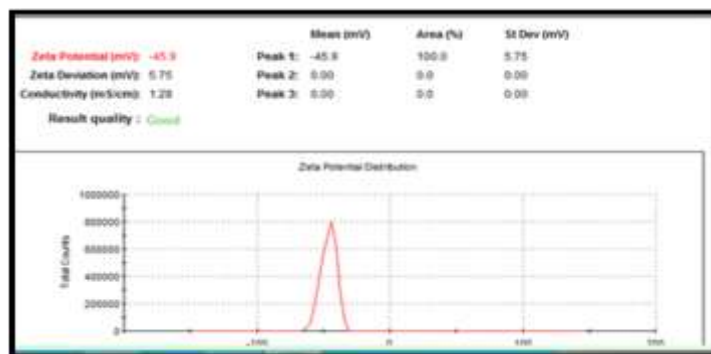


Figure 2. Zeta potential of ATCNPs

Encapsulation efficiency

The percentage encapsulation efficiency value depends upon the structure of molecule, type of technique involved, the chemical nature of encapsulating materials and dielectric constant of medium of nanoparticles synthesis [21, 24]. The percentage encapsulation efficiency was calculated using UV spectroscopy of supernatant having unbound drug in order to determine the percent of bound drug and was found to be 78.1% for Acronine and 78.4 % for TAM. Acronine and TAM are non polar hydrophobic in nature. They are greatly soluble in ethanol. Due to hydrophobic nature of Chitosan, there was a high affinity between Chitosan, Acronine and TAM. This same nature affinity resulted in increased encapsulation entrapment efficiency of the drug in Chitosan.

Morphological characterization of ATCNPs by TEM and SEM

The ACTNPs were segregated and uniformly spherical with size range of 55 – 78 nm as revealed by TEM (Figure 3A). The size dimension of nanorange particles affects drug release rate [25, 26]. NPs undergo distribution to different concentration to various body organs according to their shape & size. The relative stability, biocompatibility with natural body environment and penetration of nanoparticles inside the cell plasma membrane are likewise governed by morphology & size of nanoparticles [26]. Nanoparticles range particles are maintained systemic circulation for a longer period as comparison with large size nanoparticles [27]. SEM image analysis confirmed that the nanoparticles have spherical in shapes (Figure 3 B).

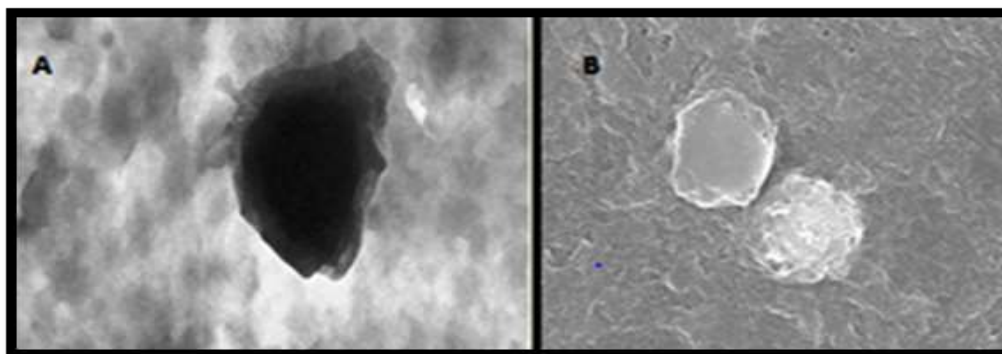


Figure 3: TEM and SEM image of ATCNPs

FTIR Analysis of Drug Samples

The FTIR spectroscopy is used to study both the interaction [27] and evaluation of the nanoencapsulation of bioactive molecules [28]. The FTIR spectra of pure drug Acronine and TAM, Chitosan and ATCNPs are shown in Figure 4. The FTIR spectrum of Acronine showed absorption peak bands at 3226 cm^{-1} for the -OH and 2965 cm^{-1} & 2412 cm^{-1} for the terminal $-\text{CH}_3$ groups. The FTIR spectrum of TAM in Figure 4 B showed characteristic absorption band for $=\text{C-H}$ stretching at 2896 cm^{-1} and 1613 cm^{-1} for $\text{C}=\text{C}$ ring stretching. The value of wave number at 1452 cm^{-1} and 3377 cm^{-1} signified $-\text{NH}_2$ stretch. The FTIR spectrum of Chitosan in Figure 4 C showed the FTIR peak at 3416 cm^{-1} for $-\text{OH}$ stretch and peak at 2934 cm^{-1} indicate aliphatic $-\text{CH}$ stretch of Chitosan. Figure 4 D representing the FTIR spectrum of ATCNPs showed variations between wave numbers 3308 cm^{-1} , 1465 cm^{-1} , 2448 cm^{-1} and 2918 cm^{-1} in ATCNPs. This region is the IR stretching vibration zone of functional groups like $-\text{OH}$, $\text{C}=\text{C}$ Stretch, $-\text{CH}_3$ Stretch and the C-H stretch. The weak-physical bonds such as dipole-dipole interaction, hydrogen bonding and weak Van der Waals forces take place between the C-H present in the drug molecule and OH present in Chitosan. The drugs & excipients revealed characteristic peaks in FTIR spectrum. The decrease in peak intensity and bands were shifted, confirmed presence of physical interaction among Acronine and TAM, Chitosan.

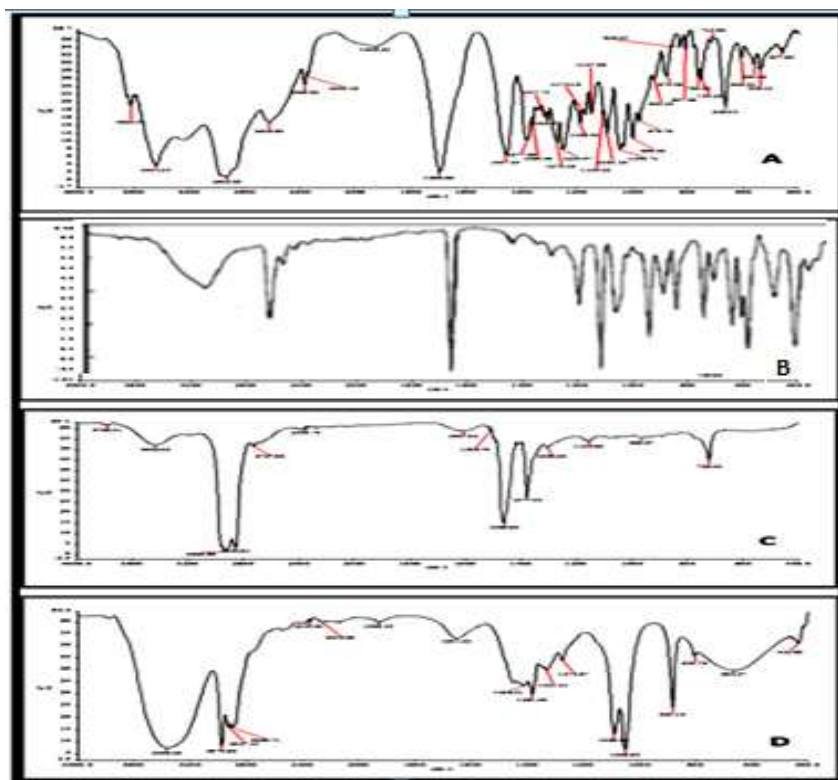


Figure 4. The FTIR spectra of pure drug (A) Acronine, (B) TAM, (C) Chitosan, (D) ATCNPs

In-vitro drug release

The persistent release of bioactive natural potent molecules out of nanoparticles cage made of Chitosan protects it from rapid metabolism and degradation [29]. Figure 5 shows the *in vitro* drug release profile of Acronine and TAM and ATCNPs. The *in-vitro* drug release data showed that 89% of the pure Acronine and 90% of pure TAM was released in 6h only, while the ATCNPs exhibited sustained release of the drug due to high better and efficient entrapments of drug in Chitosan. The ATCNPs showed release of 16% Acronine and 20% TAM after 1 h of administration. After 24 h, 72% of Acronine and 82% TAM was released from ATCNPs. Overall drug release of ATCNPs showed sustained release profile of Acronine and TAM with the passage of time which is due to hydrophobic (nonpolar) nature of Acronine and TAM. Chitosan also create a thick, strong walled and dense matrix around the Acronine and TAM particles thus ensuring its sustained release (30).

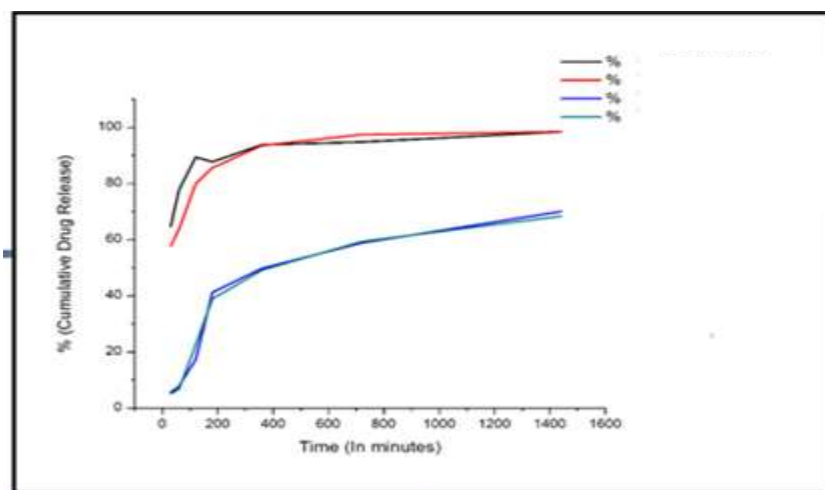


Figure 5. In-vitro release study

HPLC Conditions:

- 1 Equipment Model: Agilent 1200 Infinity Series
- 2 Column: ZORBAX SB C-18, Dimension(mm): 150 x 4.6; Particle size(μ): 5;
- 3 Detector: DAD
- 4 Pump: Isocratic
- 5 Mobile Phase: Acetonitrile: Water (80:20)
- 6 Flow Rate: 1 ml/min
- 7 Wavelength: Betulinic acid (210 nm)
- 8 Injection volume: 2 μ l
- 9 Retention Time(min.) Betulinic acid (6.6)

HPLC Conditions:

- 1 Equipment Model: Agilent 1200 Infinity Series
- 2 Column: ZORBAX SB C-18, Dimension(mm):150 x 4.6; Particle size(μ):5;
- 3 Detector: DAD
- 4 Pump: Isocratic
- 5 Mobile Phase: Acetonitrile:Water (80:20)
- 6 Flow Rate: 1ml/min
- 7 Wavelength: Betulinicacid (210 nm)
- 8 Injection volume: 2 μ l
- 9 Retention Time(min.):Betulinicacid (6.67)

Anti-oxidant activity

The DPPH analysis is used to compare quantitatively the antioxidant potency of encapsulated molecules [31]. DPPH (1,1-diphenyl-2-picrylhydrazyl) is a stable free radical, absorbing light to show excitation and during emission emit a deep violet coloration at absorption near 517 nm [32]. The Acronine and TAM are well known antioxidant potency. Acronine and TAM were incubated with DPPH resulting in the change of violet color to pale yellow. Thus, a decrease in absorbance band was observed. The Acronine and TAM contain labile hydrogen atoms that liberation leads to inhibit DPPH. The ATCNPs exhibited higher percent inhibition of DPPH as compared to Acronine and TAM alone due to nanometric dimension with a large surface area during dark incubation that provided protection to Acronine and TAM from being oxidized (Fig 6).

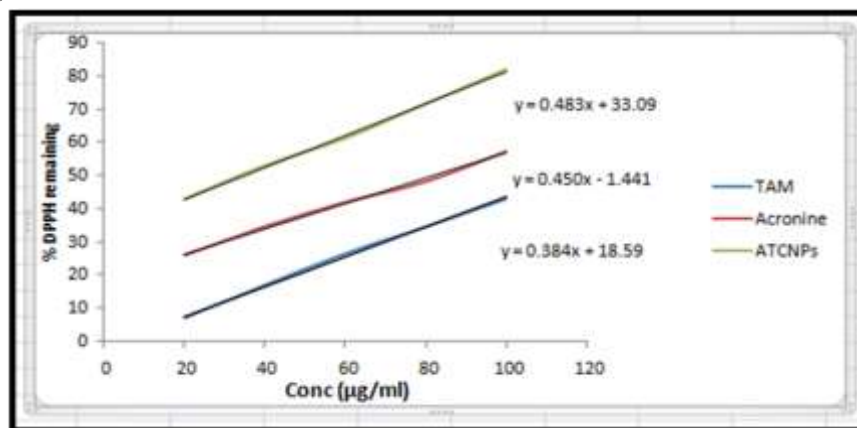


Figure 6. Antioxidant activity of Acronine, TAM and ATCNPs

Anti-cancer activity

The cytotoxic efficacy of nanoparticles represented in Figure 7 was primarily due to their greater surface area, which enabled very efficient drug delivery and antitumor activity [33]. The nano range particles are better competent to infiltrate tumor cells effectively having larger retention nature and enhanced vascular permeation [34]. Hence, NPs potency against the cancer cell lines is a function of size [35, 36]. In the, current investigation anti-cancer appetency of ATCNPs was found to be more efficient than TAM. *In vitro* study confirmed that Acronine and TAM encapsulated in Chitosan inhibited the growth of MCF-7 more effectively than the free drugs (Tamoxifen) alone. The IC₅₀ values (μ g/ml) of synthesized

nanoparticles along with standard drug tamoxifen & Acronine are given in Table 1. The results revealed that ATCNPs showed potent anticancer effect with IC₅₀ of 4.05 µg/ml, 3.97 µg/ml and 4.13 µg/ml in comparison to standard drugs TAM and Acronine alone as analyzed under optical microscope (Fig.7) against cell lines A-549 cells, MCF-7 and Hela cell lines. The potent anticancer action of ATCNPs was primarily due to the combined synergistic effect of TAM and Acronine in ATCNPs.

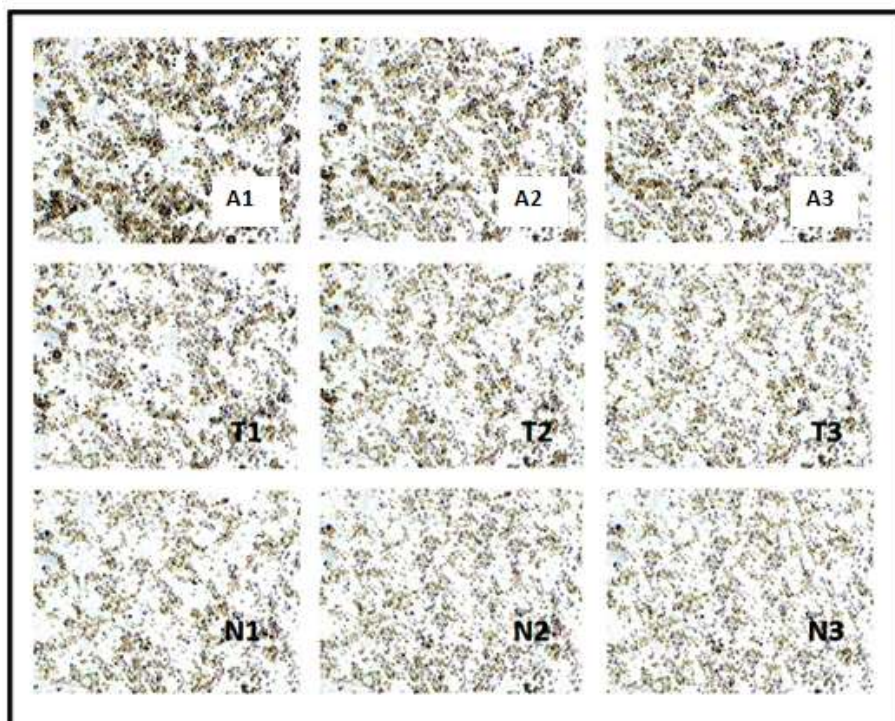


Figure 7. Optical microscope images of Cytotoxic effect of Acronine (A1, A2, and A3) TAM (T1,T2,T3) and ATCNPs (N1, N2, N3) on towards A-549, MCF-7, and Hela cell lines after 24 h.

Table 1: IC₅₀ values of ATCNPs along with standard drug Tamoxifen and Acronine

Sample code	A-549		MCF-7		Hela	
	IC ₅₀	pIC ₅₀	IC ₅₀	pIC ₅₀	IC ₅₀	pIC ₅₀
Tamoxifen	5.9	-0.7709	5.28	-0.7226	5.32	-0.7259
Acronine	26.56	-1.4238	26.36	-1.4210	29.45	-1.4683
ATCNPs	4.05	-0.6075	3.97	-0.6096	4.13	-0.6160

Conclusions

Nanomedicine and nano delivery systems are a relatively new but rapidly developing science where materials in the nanoscale range are employed to serve as means of diagnostic tools or to deliver therapeutic agents to specific targeted sites in a controlled manner. Initially, the use of nanotechnology was largely based on enhancing the solubility, absorption, bioavailability, and controlled-release of drugs. The efficacy of Acronine and TAM has greatly improved through the use of nanocarriers formulated with Chitosan. Nanoparticles have a greater potency because of their novel natural biomaterials for their quality of being biodegradable, biocompatible, readily availability, renewable and low toxicity. Thus it is important to develop novel nanoformulations consisting more powerful excipients in order to enhance solubility in water, bioavailability to blood from intestine, therapeutic potential to kill cancer cell lines and to reduced dosage. In the current study, the synergistic antioxidant as well as anticancer potential of novel nanoformulation containing Acronine co-delivered TAM loaded Chitosan nanoparticles based on dual drug delivery approach have emerging as promising molecule to combat cancer effectively.

Conflict of Interest

There is no conflict of interest.

REFERENCES

1. Tripathi, S., Sanjeevi, R., Anuradha, J., Chauhan, D. S. & Rathoure, A. K. (2022). Nano-bioremediation: nanotechnology and bioremediation. In Research Anthology on Emerging Techniques in Environmental Remediation (pp. 135-149). IGI Global.
2. Zhang, L. G., Leong, K. & Fisher, J. P. (Eds.). (2022). 3D bioprinting and nanotechnology in tissue engineering and regenerative medicine. Academic press.
3. Ferdows, B. E., Patel, D. N., Chen, W., Huang, X., Kong, N. & Tao, W. (2022). RNA cancer nanomedicine: nanotechnology-mediated RNA therapy. *Nanoscale*, **14**(12), 4448-4455.
4. Seca, A. M. & Pinto, D. C. (2018). Plant secondary metabolites as anticancer agents: successes in clinical trials and therapeutic application. *International journal of molecular sciences*, **19**(1), 263.
5. Brown, D. W., Adams, T. H. & Keller, N. P. (1996). *Aspergillus* has distinct fatty acid syntheses for primary and secondary metabolism. *Proceedings of the National Academy of Sciences*, **93**(25), 14873-14877.
6. Neto, M. R. F., DaCosta, J. B. N., Sant'Anna, C. M. R. & Carneiro, J. W. M. (2005). Structure-activity relationship studies of new acronine analogues as suggested by molecular descriptors. *Arznei mittel forschung*, **55**(05), 282-288.
7. Gottselig, N., Nischwitz, V., Meyn, T., Amelung, W., Bol, R., Halle, C. & Klumpp, E. (2017). Phosphorus binding to nanoparticles and colloids in forest stream waters. *Vadose Zone Journal*, **16**(3), 1-12.
8. Tran, T. D., Olsson, M. A., McMillan, D. J., Cullen, J. K., Parsons, P. G., Reddell, P. W. & Ogbourne, S. M. (2020). Potent antibacterial prenylated acetophenones from the Australian endemic plant *Acronychia crassipetala*. *Antibiotics*, **9**(8), 487.

9. Epifano, F., Fiorito, S. & Genovese, S. (2013). Phytochemistry and pharmacognosy of the genus *Acronychia*. *Phytochemistry*, **95**, 12-18.
10. Scarffe, J. H., Beaumont, A. R. & Crowther, D. (1983). Phase 1-11 Evaluation of Acronine in Patients With Multiple Myeloma? *Cancer treatment reports*, **67**(1), 93.
11. Kanhere, S. S., Vyas, A. H., Bhat, C. V., Kamath, B. R., Shah, R. S. & Bafna, S. L. (1969). Studies with ion- exchange resins on cinchona alkaloids III: Exchange rates. *Journal of pharmaceutical sciences*, **58**(12), 1550-1552.
12. Tran, T. D., Olsson, M. A., McMillan, D. J., Cullen, J. K., Parsons, P. G., Reddell, P. W. & Ogbourne, S. M. (2020). Potent antibacterial prenylated acetophenones from the australian endemic plant *Acronychia crassipetala*. *Antibiotics*, **9**(8), 487.
13. Ogawa, K., Yui, T. & Okuyama, K. (2004). Three D structures of chitosan. *International Journal of Biological Macromolecules*, **34**(1-2), 1-8.
14. Mourya, V. K., & Inamdar, N. N. (2008). Chitosan-modifications and applications: Opportunities galore. *Reactive and Functional polymers*, **68**(6), 1013-1051.
15. Li, Q., Dunn, E. T., Grandmaison, E. W. & Goosen, M. F. (2020). Applications and properties of chitosan. In *Applications of chitin and chitosan* (pp. 3-29). CRC Press.
16. Li, J., Lee, I. W., Shin, G. H., Chen, X. & Park, H. J. (2015). Curcumin-Eudragit® E PO solid dispersion: a simple and potent method to solve the problems of curcumin. *European Journal of Pharmaceutics and Biopharmaceutics*, **94**, 322-332.
17. Osborne, C. K. (1998). Tamoxifen in the treatment of breast cancer. *New England Journal of Medicine*, **339**(22), 1609-1618.
18. Jordan, V. C. (2003). Tamoxifen: a most unlikely pioneering medicine. *Nature reviews Drug discovery*, **2**(3), 205-213.
19. Bradley, R., Braybrooke, J., Gray, R., Hills, R. K., Liu, Z., Pan, H. & Swain, S. M. (2022). Aromatase inhibitors versus tamoxifen in premenopausal women with oestrogen receptor-positive early-stage breast cancer treated with ovarian suppression: a patient-level meta-analysis of 7030 women from four randomised trials. *The Lancet Oncology*, **23**(3), 382-392.
20. Shrivastava, N., Parikh, A., Dewangan, R. P., Biswas, L., Verma, A. K., Mittal, S. & Baboota, S. (2022). Solid Self-Nano emulsifying nanoplatform loaded with Tamoxifen and Resveratrol for treatment of breast cancer. *Pharmaceutics*, **14**(7), 1486.
21. Iqbal, M., Zafar, N., Fessi, H. & Elaissari, A. (2015). Double emulsion solvent evaporation techniques used for drug encapsulation. *International journal of pharmaceutics*, **496**(2), 173-190.
22. Antolovich, M., Prenzler, P. D., Patsalides, E., McDonald, S. & Robards, K. (2002). Methods for testing antioxidant activity. *Analyst*, **127**(1), 183-198.
23. Meerloo, J. V., Kaspers, G. J. & Cloos, J. (2011). Cell sensitivity assays: the MTT assay. In *Cancer cell culture* (pp. 237-245). Humana Press.
24. Jyothi, N. V. N., Prasanna, P. M., Sakarkar, S. N., Prabha, K. S., Ramaiah, P. S. & Srawan, G. Y. (2010). Microencapsulation techniques, factors influencing encapsulation efficiency. *Journal of microencapsulation*, **27**(3), 187-197.

25. Mayeen, A., Shaji, L. K., Nair, A. K. & Kalarikkal, N. (2018). Morphological characterization of nanomaterials. In *Characterization of Nanomaterials* (pp. 335-364). Woodhead Publishing.
26. Bartoov, B., Eltes, F., Weissenberg, R. & Lunenfeld, B. (1980). Morphological characterization of abnormal human spermatozoa using transmission electron microscopy. *Archives of Andrology*, **5**(4), 305-322.
27. Aprea, G., D'Angelo, A. R., Prencipe, V. A. & Migliorati, G. (2015). Bacteriophage morphological characterization by using transmission electron microscopy. *Journal of Life Sciences*, **9**(1), 214-220.
28. Beganskienė, A., Sirutkaitis, V., Kurtinaitienė, M., Juškėnas, R. & Kareiva, A. (2004). FTIR, TEM and NMR investigations of Stöber silica nanoparticles. *Mater Sci (Medžiagotyra)*, **10**, 287-290.
29. Singhvi, G., & Singh, M. (2011). In-vitro drug release characterization models. *International Journal of Pharma Study Research*, **2**(1), 77-84.
30. Svensson, O., Lindh, L., Cárdenas, M., & Arnebrant, T. (2006). Layer-by-layer assembly of mucin and chitosan—Influence of surface properties, concentration and type of mucin. *Journal of colloid and interface science*, **299**(2), 608-616.
31. Sirivibulkovit, K., Nouanthavong, S., & Sameenoi, Y. (2018). Based DPPH assay for antioxidant activity analysis. *Analytical sciences*, **34**(7), 795-800.
32. Goupy, P., Dufour, C., Loonis, M., & Dangles, O. (2003). Quantitative kinetic analysis of hydrogen transfer reactions from dietary polyphenols to the DPPH radical. *Journal of Agricultural and Food Chemistry*, **51**(3), 615-622.
33. Chen, Z., Tai, Z., Gu, F., Hu, C., Zhu, Q. & Gao, S. (2016). Aptamer-mediated delivery of docetaxel to prostate cancer through polymeric nanoparticles for enhancement of antitumor efficacy. *European Journal of Pharmaceutics and Biopharmaceutics*, **107**, 130-141.
34. Xu, Z., Chen, L., Gu, W., Gao, Y., Lin, L., Zhang, Z. & Li, Y. (2009). The performance of docetaxel-loaded solid lipid nanoparticles targeted to hepatocellular carcinoma. *Biomaterials*, **30**(2), 226-232.
35. Li, S., Feng, X., Wang, J., Xu, W., Islam, M. A., Sun, T. & Chen, X. (2019). Multiantigenic nanoformulations activate anticancer immunity depending on size. *Advanced Functional Materials*, **29**(49), 1903391-400.
36. Miao, L., Guo, S., Lin, C. M., Liu, Q. & Huang, L. (2017). Nanoformulations for combination or cascade anticancer therapy. *Advanced drug delivery reviews*, **115**, 3-22.